Sulfide Capacity of Molten $CaO-SiO_2-MnO-Al_2O_3-MgO$ Slags

Joo Hyun PARK[1),] and Geun-Ho PARK[1,2)]*

1) School of Materials Science and Engineering, University of Ulsan, Ulsan 680-749, Korea

2) Steelmaking Technology Development Team, Technical Research Center, Hyundai Steel Corp., Dangjin, Korea

Abstract: The sulfide capacities of the $CaO–SiO_2–MnO–Al_2O_3$–5wt% MgO slags were measured at 1873 K over a wide composition range using a gas–slag equilibration method. The effects of basicity and the activity coefficient of sulfide on the sulfide capacity of molten slag were also investigated based on the structural view of silicate melts. In the multicomponent silicate melts containing high MnO (up to about 50wt%), the sulfide capacity mainly increased with increasing MnO content. The capacity and modified Vee ratio, *i.e.* $(CaO+MnO+MgO)/(SiO_2+Al_2O_3)$, showed a good linear relationship. Assuming that the basicity and the stability of sulfide ions in the slag are proportional to the activity of basic oxides and the activity coefficient of sulfides, the composition dependency of the sulfide capacity is well described by changes in the a_{MO} to γ_{MS} (M=Ca, Mn) ratio. The substitution of silica by alumina did not affect the sulfide capacity of the slags not only because of an increase in the activity of basic oxides but also because of a decrease in the stability of sulfides as Al_2O_3/SiO_2 ratio increased. In the high silica melts of which silica content greater than about 30wt%, the sulfide capacity increased with increasing MnO/CaO ratio, whereas it decreased by increasing the MnO/CaO ratio in the low silica melts (< about 30wt%). This tendency of sulfide capacity resulted in the clock–wisely rotating iso–capacity contours in the $CaO–SiO_2–MnO–Al_2O_3–MgO$ system at 1873 K. The competitive dissolution mechanism of sulfur in the MnO–containing calcium silicate melts can be explained not only by the difference in the structural role of Ca^{2+} and Mn^{2+} ions but also by the changes in the content of O^{2-} ions according to the silica content.

Key words: Sulfide capacity, $CaO–SiO_2–MnO–Al_2O_3–MgO$ slag, Basicity, Sulfide stability, Silicate structure, Competitive sulfur dissolution mechanism.

1. Introduction

Desulfurization has been emphasized over several decades in iron- and steelmaking processes.[1–7] Sulfur is harmful to the mechanical properties of steel products (e.g., strength, ductility and toughness). Therefore, it is necessary to remove sulfur from molten steel to under several ppm in order to improve mechanical properties. Additionally, the demand for ferrous and non-ferrous manganese alloys has increased continuously due to the introduction of advanced high strength steels such as TRIP and TWIP aided steels that were recently developed to contain manganese up to about 30wt%.[8–12] Thus, the desulfurization of manganese (ferro–)alloys and high manganese steels is an important issue.

Even though many researchers have investigated the sulfide capacities of molten slags, there are few experimental data regarding high MnO–containing multicomponent slags. We recently investigated experimental and modeling approaches for the $CaO–SiO_2–MnO$ ternary system.[6–7] In the present paper, we focus on sulfur dissolution behavior

into multicomponent calcium manganosilicate melts containing Al_2O_3 and MgO.

Nzotta et al.[13] measured the sulfide capacities of the CaO–SiO_2–MnO–Al_2O_3 quaternary system at temperatures from 1773 to 1923 K by a gas–slag equilibration method and proposed iso–sulfide capacity contours calculated from their KTH model for the system of X_{CaO} = 0.13. In their modeling results, the sulfide capacity of the slags dominantly increased by increasing the MnO content, independent of the Al_2O_3/SiO_2 ratio. The effect of MnO on the sulfide capacity of low–silica (6~8wt%) CaO–Al_2O_3–MnO–SiO_2 slags was the same.[2] Nzotta[14] and Nilsson et al.[15] also measured the sulfide capacities of the CaO–SiO_2–MnO–MgO slags at temperatures from 1773 to 1923 K to develop model parameters based on experimental data. They proposed iso–sulfide capacity contours that were calculated from the KTH model of X_{MnO} = 0.05 system. In their modeling results, the sulfide capacity of the slags were strongly decreased by increasing the silica content and moderately decreased with increasing MgO/CaO ratio at given silica and alumina contents.

The sulfide capacities of the CaO–SiO_2–MnO–Al_2O_3–MgO quinary system were measured by Seetharaman et al.[13,15] In these studies, the sulfide capacities of the six composition systems were measured at temperatures from 1773 to 1923 K. The calculated sulfide capacity of the 5 component slags with X_{CaO} = 0.07 and X_{MgO} = 0.36 generally increased with increasing MnO content, with a minimum at about $X_{Al_2O_3}$ = 0.1 at a fixed MnO/SiO_2 ratio. In more recent work by Taniguchi et al.[2], the sulfide capacities of low–silica (3~11wt%) CaO–Al_2O_3–MnO–SiO_2–4wt% MgO slags were measured at 1673 to 1723 K. Manganese oxide increased the sulfide capacities of slags, with its addition being more effective at lower temperatures. The addition of MgO (4wt%) increased the sulfide capacities of slags in the 0~10wt% MnO range, but there was no substantial effect above 10wt% MnO.

Therefore, in the present study we measured the sulfide capacities of the CaO–SiO_2–MnO–Al_2O_3–5wt% MgO slags at 1873 K through a wide composition range, and also discussed the thermodynamic effects of basicity and the stability of sulfide on the dissolution behavior of sulfur into the CaO–SiO_2–MnO–Al_2O_3–MgO slags.

2. Experimental Procedure

A super–kanthal vertical electric resistance furnace was used for the equilibration between the CaO–SiO_2–MnO–Al_2O_3–MgO slag and gas phase at 1873 K. The temperature was controlled within ±2 K using an installed B–type thermocouple and a PID controller. The furnace temperature was also calibrated using an external B–type thermocouple before experiment. The slag samples were prepared using reagent–grade SiO_2, MnO, Al_2O_3, MgO and CaO calcined form $CaCO_3$ at 1273 K. The slag sample of 1.2 g was maintained in a Pt crucible which was held in the porous alumina holder under the CO–CO_2–SO_2–Ar gas mixture for 8 hours. A constant flow rate of 400 ml/min was maintained during the equilibration of the slag with gas mixture at the experimental temperature. The schematic diagram of the experimental apparatus is shown in Figure 1.

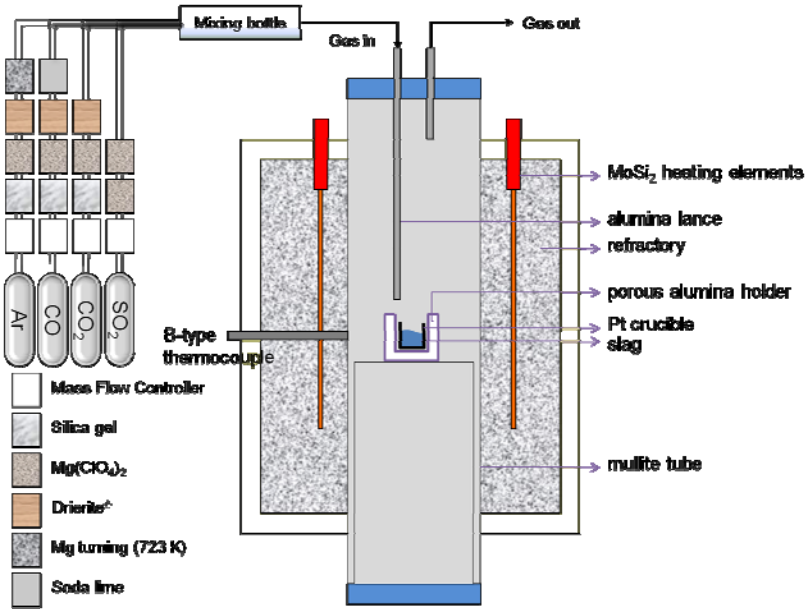

Fig.1 Schematic diagram of the experimental apparatus.

Each gas was passed through the purification system to remove the impurities. The oxygen partial pressure was calculated by Eq. [1], and the partial pressure of gaseous sulfur was obtained from Eq. [3] by incorporating the oxygen partial pressure determined from Eq. [2].[16]

$$CO_2(g) = CO(g) + \frac{1}{2}O_2(g), \quad \Delta G^o_{[1]} = 281100 - 85.3\,T \quad \text{(J/mol)} \qquad [1]$$

$$K_{[1]} = \frac{p_{CO} \cdot p_{O_2}^{1/2}}{p_{CO_2}} = \exp\left(-\frac{\Delta G^o_{[1]}}{RT}\right) \qquad [2]$$

$$SO_2(g) = \frac{1}{2}S_2(g) + O_2(g), \quad \Delta G^o_{[3]} = 361800 - 72.7\,T \quad \text{(J/mol)} \qquad [3]$$

$$K_{[3]} = \frac{p_{S_2}^{1/2} \cdot p_{O_2}}{p_{SO_2}} = \exp\left(-\frac{\Delta G^o_{[3]}}{RT}\right) \qquad [4]$$

The flow rate of each gas and the calculated oxygen and sulfur potentials are listed in Table 1.

After equilibration, the sample was quickly drawn from the furnace and then quenched by dipping it into brine. The quenched samples were crushed to less than 100 μm using stainless and agate mortars for chemical analysis. The content of sulfur and each component in the slag were determined by combustion analyzer and XRF spectroscopy,

respectively. The activity of each component in slag phase was calculated by commercial thermochemical computing program, FactSage6.2™ with 'FToxid' database.[17] This database was successfully used for the estimation of the thermodynamic properties of oxide systems through a wide temperature and composition range.[1,6,7,18–31]

Table 1 Mass flow of each gas and calculated oxygen and sulfur partial pressures.

Mass flow of gas phases (ml/min)					Gas potential (atm)	
CO	CO_2	SO_2	Ar	Total	p_{O_2}	p_{S_2}
125	160	15	100	400	2.80×10^{-7}	4.71×10^{-3}

3. Results and Discussion

3.1 Effect of MnO content on sulfide capacity of $CaO–SiO_2–MnO–Al_2O_3–MgO$ slags

The experimental compositions were designed to elucidate the effect of MnO at a given Vee ratio (= CaO/SiO_2 = 1.1 and 0.5) and to study the replacement effect of CaO by MnO at a fixed silica content (40wt%) and the substitution effect of alumina for silica at a fixed CaO and MnO contents. Figure 2 shows the effect of MnO content on the sulfide capacity of the $CaO–SiO_2–MnO–20wt\%\ Al_2O_3–5wt\%$ MgO slags at 1873 K under each condition. The sulfide capacity increases with increasing MnO content, indicating that MnO behaves as a basic oxide in the present slag system. Also, the higher the Vee ratio, the greater the capacity is obtained at a given MnO content, which is in good agreement with theoretical expectations. It seems that sulfide capacity slightly increases by increasing the MnO/CaO ratio at 40wt% SiO_2 from MnO–free to CaO–free systems. The experimental data for the $CaO–SiO_2–MnO$ ternary slag system at 1873 K is also shown in Figure 1.[6] It is interesting that the sulfide capacity of the ternary and quinary slags are not so much different at the similar C/S condition, although it seems that the capacity of the quinary slag at C/S=1.0 is slightly higher than that of ternary system at low MnO content.

Figure 3 shows the relationship between the sulfide capacity of the $CaO–SiO_2–MnO–Al_2O_3–MgO$ slags at 1873 K and the mass ratio of $(MnO+CaO+MgO)/(SiO_2+Al_2O_3)$, including the reference data from Taniguchi et al.[2] at 1673 and 1773 K. The sulfide capacity of the $CaO–SiO_2–MnO$ ternary slag at 1873 K is also compared.[6] Even though the simple Vee ratio has been widely used to evaluate the basicity of slags, the modified Vee ratio shows a good composition dependency of the sulfide capacity in the $CaO–SiO_2–MnO$ ternary and the $CaO–SiO_2–MnO–Al_2O_3–MgO$ quinary slags. Comparing both experimental data, the sulfide capacity of the low–silica (3~11wt%) slag systems is similar to that of the relatively high–silica (18~49wt%) slag systems, even though the experimental temperature of the former is about 100 to 200 K lower than that of the latter. This is in good correspondence to the sulfide capacity difference in between calcium silicates and calcium aluminates.[6,32–34]

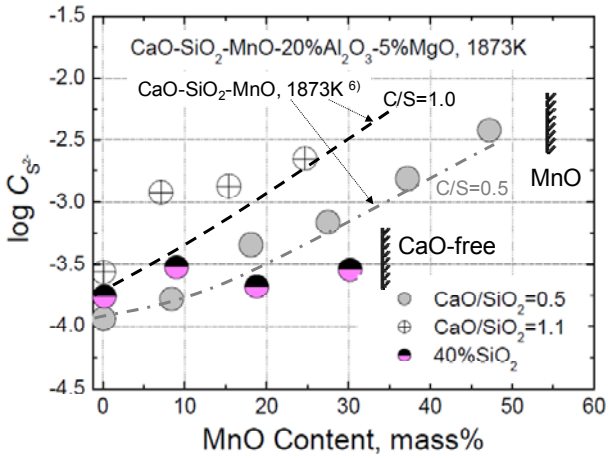

Fig.2 Effect of MnO on the sulfide capacity of the slags at (%CaO)/(%SiO_2) = 0.5 and 1.1, and at 40wt% SiO_2.

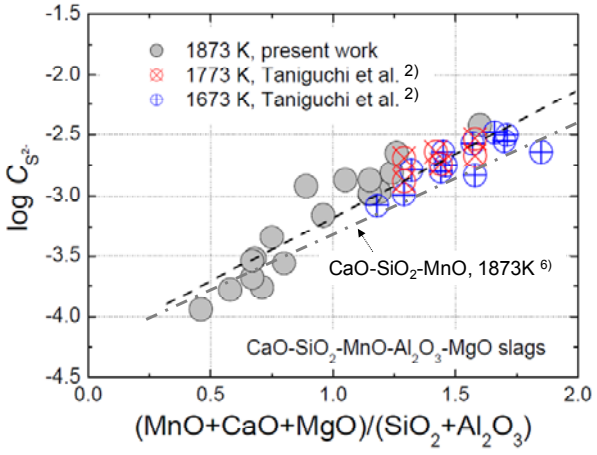

Fig.3 Relationship between the (MnO+CaO+MgO)/(SiO_2+Al_2O_3) ratio and sulfide capacity of slags.

3.2 Effect of MnO activity on sulfide capacity of CaO–SiO_2–MnO–Al_2O_3–5%MgO slags

The sulfide capacity of the CaO–SiO_2–MnO–Al_2O_3–5wt% MgO slags at 1873 K is plotted in Figure 4 against the activity of MnO on a logarithmic scale. Based on a definition of sulfide capacity, Eq. [6],[32] it is expected to be proportional to the activity of O^{2-} ion in a logarithmic scale as indicated in Eq. [7] assuming that the activity coefficient of S^{2-} ion is not significantly affected by slag composition.

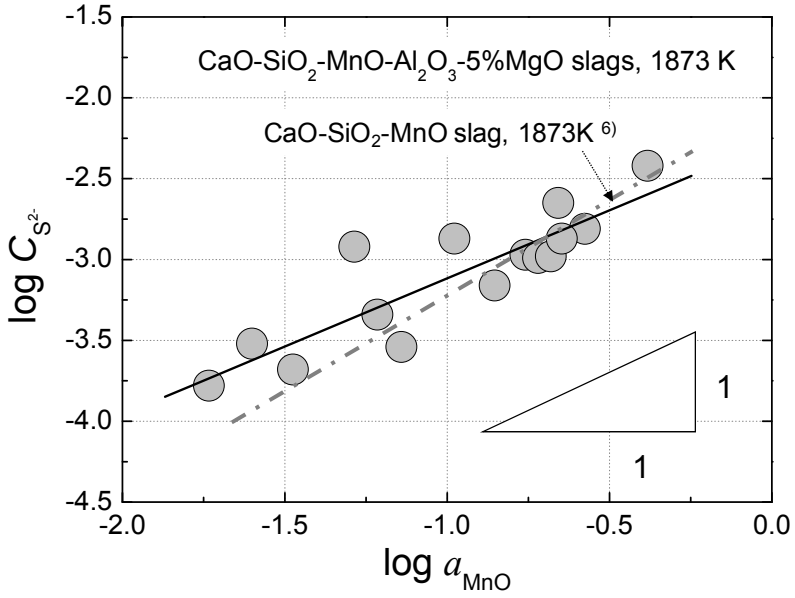

Fig.4 Relationship between the activity of MnO and the sulfide capacity of slags at 1873 K.

$$\frac{1}{2}S_2(g) + (O^{2-}) = (S^{2-}) + \frac{1}{2}O_2(g) \quad [5]$$

$$C_{S^{2-}} \equiv \frac{K_{[5]} \cdot a_{O^{2-}}}{f_{S^{2-}}} = (\text{wt\%S}) \cdot \left(\frac{p_{O_2}}{p_{S_2}} \right)^{0.5} \quad [6]$$

$$\log C_{S^{2-}} = \log a_{O^{2-}} - \log f_{S^{2-}} + \log K_{[5]} \quad [7]$$

where $K_{[5]}$ is the equilibrium constant of Eq. [5], $a_{O^{2-}}$ is the activity of O^{2-} ion, and $f_{S^{2-}}$ is the Henrian activity coefficient of S^{2-} ion in the slag. However, due to thermodynamic restriction, the activity of basic oxide is assumed to be proportional to that of O^{2-} ion based on Eqs. [8] and [9].

$$(MnO) = (Mn^{2+}) + (O^{2-}) \quad [8]$$

$$\log a_{MnO} = \log a_{O^{2-}} + \log a_{Mn^{2+}} - \log K_{[8]} \quad [9]$$

By combining Eqs. [7] and [9], the following relationship can be deduced.

$$\log C_{S^{2-}} = \log a_{MnO} - \log a_{Mn^{2+}} - \log f_{S^{2-}} + C \quad [10]$$

where C may be assumed less sensitive to slag composition. As shown in Figure 4, there is a linear correlation between $\log C_{S^{2-}}$ and $\log a_{MnO}$ with the slope of about 0.84 (obtained from a linear regression analysis), which is relatively close to the theoretical value of unity within experimental scatters. This means that an increasing rate of $a_{Mn^{2+}}$ would be balanced with a decreasing rate of $f_{S^{2-}}$ as the activity of MnO increases.

3.3 Effect of Al_2O_3/SiO_2 substitution on sulfide capacity of 20%CaO–30%MnO–5%MgO–SiO_2–Al_2O_3 slags

Sulfide capacity does not change by the substitution of alumina for silica at a given Al_2O_3+SiO_2(=45wt%) condition as shown in Figure 5. Here, the contents of MnO and CaO were fixed at 30 and 20wt%, respectively. This is in good agreement with the result of Nzotta et al.[13] for the CaO–MnO–SiO_2–Al_2O_3 (X_{CaO} = 0.13) system. Because the

effect of sulfide stability on capacity must be independently investigated, we incorporated the activity coefficient of MS (M=Ca, Mn) calculated from Eq. [12] into the thermodynamic assessment as follows.[3,7]

$$\mathrm{MO(l)} + \frac{1}{2}\mathrm{S_2(g)} = \mathrm{MS(l)} + \frac{1}{2}\mathrm{O_2(g)},$$

$$\Delta G^{o}_{[11]} = 66\,300 \text{ J/mol (for Ca)}, \quad 83\,800 \text{ J/mol (for Mn)} \qquad [11]$$

$$\log \gamma_{\mathrm{MS}} = -\frac{\Delta G^{o}_{[11]}}{2.303RT} + \log a_{\mathrm{MO}} - \frac{1}{2}\log\left(\frac{p_{\mathrm{O_2}}}{p_{\mathrm{S_2}}}\right) - \log X_{\mathrm{MS}} \qquad [12]$$

where γ_{MS} and X_{MS} are the activity coefficient and the mole fraction of MS in molten slag, a_{MO} is the activity of MO, and p_{i} is the partial pressure of gaseous component *i*.

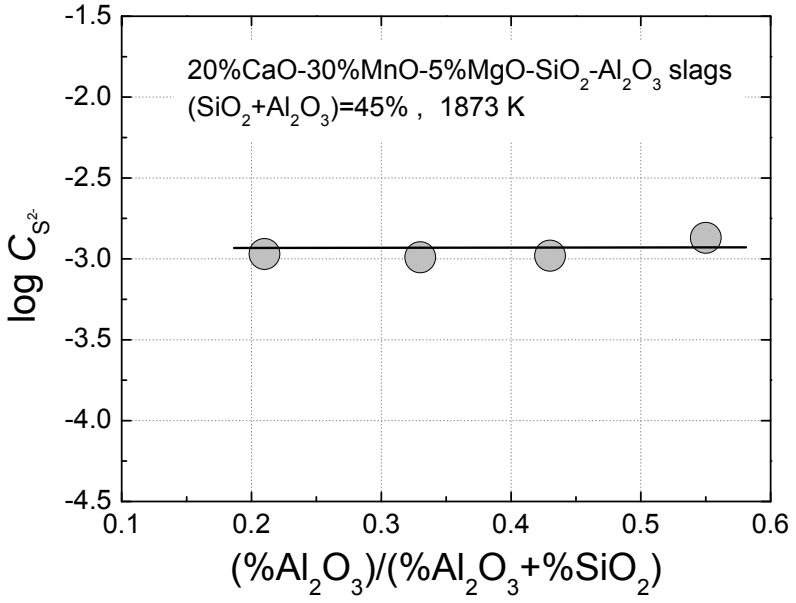

Fig. 5 Effect of the $(\%Al_2O_3)/(\%Al_2O_3+\%SiO_2)$ ratio on the sulfide capacity of the slags at 1873 K.

Figure 6 shows the activity of basic oxides such as CaO and MnO, and the activity coefficient of CaS and MnS as a function of $Al_2O_3/(Al_2O_3+SiO_2)$(=A/(A+S)) ratio, assuming that the sulfur is stabilized by totally Ca^{2+} or totally Mn^{2+} ions as an extreme condition at this composition range. However, the more detailed discussion will be given in the following section. The activity of basic oxides ($\log a_{\mathrm{CaO}}$, $\log a_{\mathrm{MnO}}$) and the activity coefficient of sulfides ($\log \gamma_{\mathrm{CaS}}$,

$\log \gamma_{MnS}$) both increase with increasing A/(A+S) ratio. It is unambiguous that the activity of basic oxides increases by decreasing the amount of SiO_2. Furthermore, the recent investigation of Lee et al.[35,36] in regard of phase equilibria of the MnO–MnS–SiO_2–Al_2O_3 and the CaO–CaS–SiO_2–Al_2O_3 systems, wherein the solubility of MnS or CaS decreased by alumina addition at a given MnO/SiO_2 or CaO/SiO_2 ratio, indicates that the activity coefficient of MnS or CaS increased with increasing alumina content. This is in good agreement to the present thermodynamic assessment. Consequently, assuming that the basicity and the stability of sulfide ions in slags are proportional to the activity of basic oxides and the activity coefficient of sulfides, respectively, a constant sulfide capacity during $Al_2O_3 \leftrightarrow SiO_2$ substitution (Figure 5) originates from the increase in both $a_{O^{2-}}$ and $f_{S^{2-}}$ in a similar degree by increasing the A/(A+S) ratio at a fixed temperature.

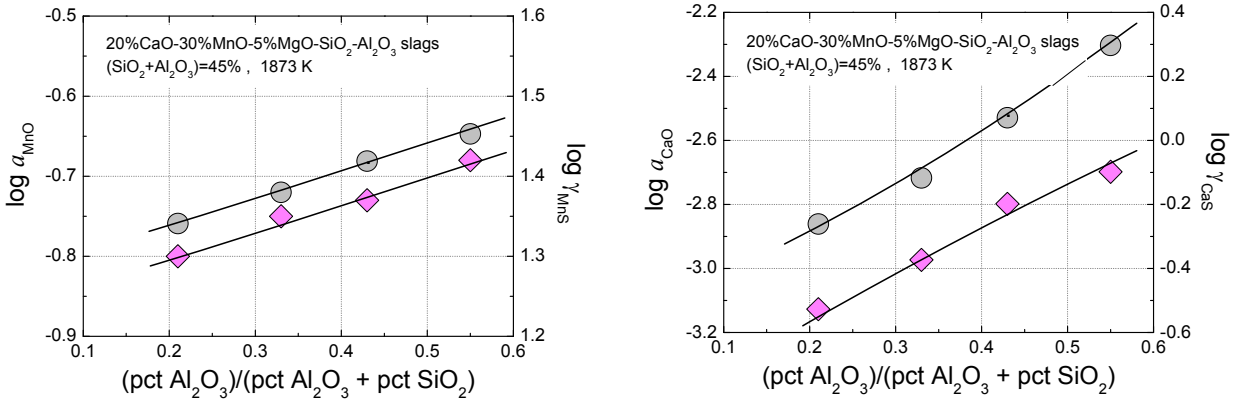

Fig. 6 The activity of basic oxides and the activity coefficient of sulfides against the (%Al_2O_3)/(%Al_2O_3+%SiO_2) ratio.

3.4 Iso-sulfide capacity of CaO–SiO_2–MnO–20%Al_2O_3–5%MgO slags

The iso–sulfide capacity of the CaO–SiO_2–MnO–20wt% Al_2O_3–5wt% MgO slags at 1873 K is shown in Figure 7. The phase diagram of the system is predicted using the FactSage™6.2 program.[17] The capacity contours seem to rotate clock–wisely from the MnO–free quaternary side to the MnO–rich corner, which is very similar tendency to that of the CaO–SiO_2–MnO ternary slag system.[6,7] Thus, the sulfide capacity increases by increasing the MnO/CaO ratio at a fixed silica content which is greater than about 35wt%, whereas it decreases by increasing the MnO/CaO ratio at silica content lower than about 35wt%. According to the authors' previous work,[6] the CaO which has more ionic bond character, *i.e.* 79% based on the Pauling's equation (Eq. [13]), dominantly contributes to the depolymerization of silicates than the MnO of which ionic bond character is 63% does.[37,38]

$$i\,(amount\ of\ ionic\ bond\ character) = 1 - e^{-\frac{1}{4}(x_A - x_B)^2} \qquad [13]$$

where x_A and x_B are, respectively, the electronegativity of A and B atoms. Hence, the large amount of Ca^{2+} cations are electrically balanced with two non–bringing oxygen ions, indicating that the Mn^{2+} cations are relatively free from the role of network modifier and mainly participate into the desulfurization reaction in high silica region. This is in good correspondence to the results shown in Figs. 2 and 7. In thermodynamic analysis using the modified quasichemical model,[7] the relative fraction of non–bringing oxygen in the silica–rich calcium silicates was greater than that in the silica–rich manganese silicate melts, resulting in the higher concentration of free oxygen in manganese silicate melts than that in calcium silicate melts, which is also shown in Figure 8(a).

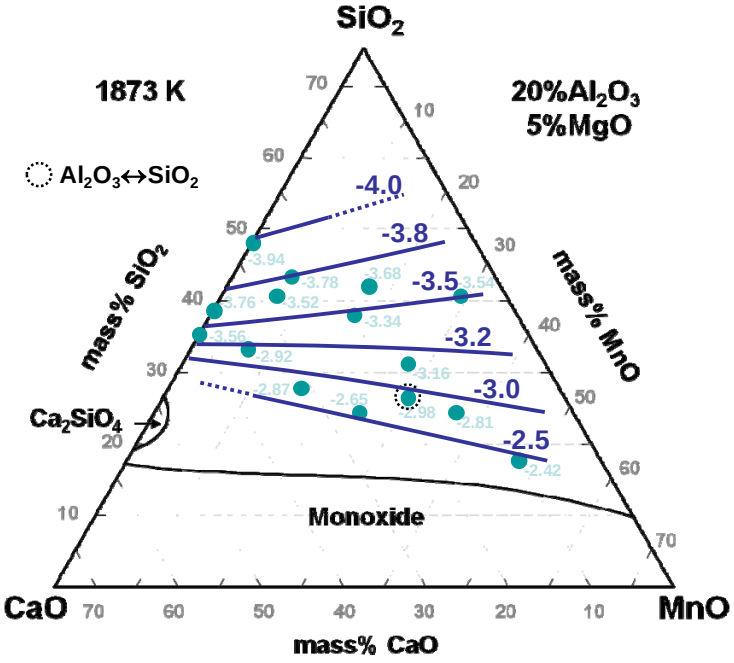

Fig. 7 Iso-sulfide capacity contours in the CaO–SiO_2–MnO–20%Al_2O_3–5%MgO slag at 1873 K.

However, in the relatively low silica region, *viz*. less than about 35wt% SiO_2, the amount of Ca^{2+} cations balancing with non–bringing oxygen is reduced and thus Ca^{2+} and Mn^{2+} cations competitively react with the S^{2-} ions, resulting in the dominant contribution of $Ca^{2+} \leftrightarrow S^{2-}$ attraction which is greater than $Mn^{2+} \leftrightarrow S^{2-}$ attraction in terms of the stability of each sulfide which was determined from the Gibbs free energy of the formation of CaS ($\Delta G^o_{f,\mathrm{CaS}} = 66.3\,\mathrm{kJ/mol}$) and MnS ($\Delta G^o_{f,\mathrm{MnS}} = 83.8\,\mathrm{kJ/mol}$) at 1873 K.[7] This indicates that the contribution of Ca^{2+} to the stabilization of S^{2-} ions would be larger than that of Mn^{2+} in the relatively low silica region. Furthermore, in thermodynamic analysis which is similar to that mentioned above, the relative fraction of free oxygen slightly decreases with increasing MnO/CaO ratio at low silica region, while that of bridging oxygen increases with MnO content as shown in Figure 8(b).

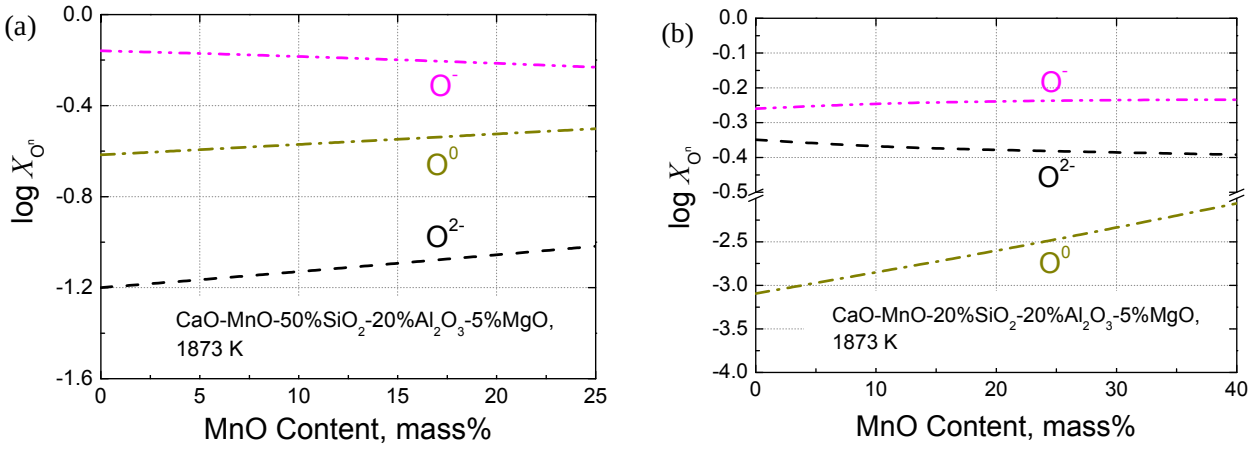

Fig. 8 Oxygen proportions in the (a) 50%SiO_2 and (b) 20%SiO_2 slags (calculated using the FactSage™6.2 program).

By combining the present results and that of previous studies,[6,7] in the high silica melts (> 30(±5)wt% SiO_2), the sulfide capacity increases with increasing MnO/CaO ratio, which originates from the fact that the content of O^{2-} ions (~ basicity) increases with increasing MnO/CaO ratio and that the stability of S^{2-} ions increases because large amounts of Ca^{2+} ions should be balanced with O^- ions, resulting in the stabilization of S^{2-} ions by interacting with Mn^{2+} ions. However, in the low silica melts (< 30(±5)wt% SiO_2), the sulfide capacity decreases with increasing MnO/CaO ratio, which originates from the fact that the content of O^{2-} ions does not change with increasing MnO/CaO ratio and that the stability of S^{2-} ions decreases because the amounts of Ca^{2+} ions balancing with O^- ions are very small, almost of S^{2-} ions are stabilized by interacting with free Ca^{2+} ions, of which amount decreases with increasing MnO/CaO ratio. Consequently, the sulfide capacity results in the clock–wisely rotating iso–capacity contours in the CaO–SiO_2–MnO(–Al_2O_3–MgO) system at 1873 K. This mechanism, which is called 'Competitive sulfur dissolution mechanism,' is schematically described in Figure 9.

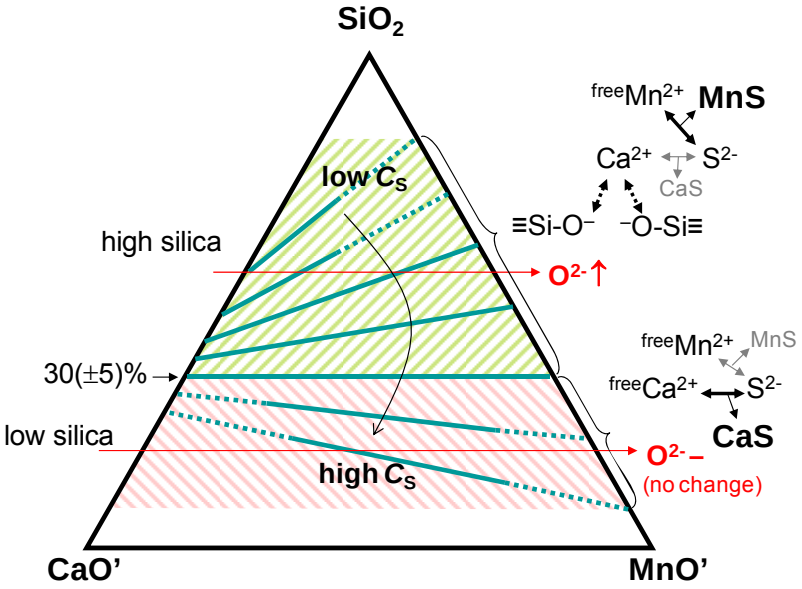

Fig. 9 The effect of slag composition on the sulfur dissolution mechanism in the CaO–MnO–SiO_2(–Al_2O_3–MgO) slags.

4. Conclusions

The sulfide capacities of the $CaO–SiO_2–MnO–Al_2O_3$–5wt% MgO slags were measured at 1873 K over a wide composition range using a gas–slag equilibration method. The effects of basicity and the activity coefficient of sulfide on the sulfide capacity of molten slag were also investigated based on the structural view of silicate melts. The specific findings of the present study are summarized below;

1) In the multicomponent silicate melts containing high MnO (up to about 50wt%), the sulfide capacity mainly increased with increasing MnO content. The capacity and modified Vee ratio, *i.e*. $(CaO+MnO+MgO)/(SiO_2+Al_2O_3)$, showed a good linear relationship in the $CaO–SiO_2–MnO–Al_2O_3$–MgO slags.

2) Assuming that the basicity and the stability of sulfide ions in the slag are proportional to the activity of basic oxides and the activity coefficient of sulfides, the composition dependency of the sulfide capacity is well described by changes in the a_{MO} to γ_{MS} (M=Ca, Mn) ratio.

3) The silica ↔ alumina substitution did not affect the sulfide capacity of the slags not only because of an increase in the activity of basic oxides but also because of a decrease in the stability of sulfides as Al_2O_3/SiO_2 ratio increases.

4) In the high silica melts (> 30(±5)wt% SiO_2), the sulfide capacity increased with increasing MnO/CaO ratio, whereas it decreased by increasing the MnO/CaO ratio in the low silica melts (<30(±5)wt% SiO_2). This tendency of sulfide capacity resulted in the clock–wisely rotating iso–sulfide capacity in the $CaO–SiO_2–MnO(–Al_2O_3–MgO)$ system at 1873 K. The dissolution mechanism of sulfur in the MnO–containing calcium silicate melts can be explained not only by the difference in the structural role of Ca^{2+} and Mn^{2+} ions but also by the changes in the content of O^{2-} ions according to the silica content.

References

[1] J.H. Park and D.J. Min. Effect of ZrO_2 Addition to the $CaO-SiO_2-MgO-CaF_2$ Slags on the Sulfur Removal from the 16Cr-14Ni Stainless Steel Melts. *Mater. Trans*., 2006, 47, p2038-2043.

[2] Y. Taniguchi, N. Sano and S. Seetharaman. Sulphide Capacities of $CaO-Al_2O_3-SiO_2-MgO-MnO$ Slags in the Temperature Range 1673-1773 K. *ISIJ Int*., 2009, 49, p156-163.

[3] Y.B. Kang and A.D. Pelton. Thermodynamic Model and Database for Sulfides Dissolved in Molten Oxide Slags. *Metall. Meter. Trans. B*, 2009, 40B, p979-994.

[4] M.K. Cho, J. Cheng, J.H. Park and D.J. Min. Hot Metal Desulfurization of $CaO-SiO_2-CaF_2-Na_2O$ Slag saturated with MgO. *ISIJ Int*., 2010, 50, p215-221.

[5] T. Tanaka, Y. Ogiso, M. Ueda and J. Lee. Trial on the Application of Capillary Phenomenon of Solid CaO to Desulfurization of Liquid Fe. *ISIJ Int*., 2010, 50, p1071-1077.

[6] G.H. Park, Y.B. Kang and J.H. Park. Sulfide capacity of the $CaO-SiO_2$-MnO slag at 1873 K. *ISIJ Int.*, 2011, 51, p1375-1382.

[7] Y.B. Kang and J.H. Park. On the dissolution behavior of sulfur in ternary silicate slags. *Metall. Meter. Trans. B*, 2011, 42B, p1211-1217.

[8] Y. Sutou, N. Kamiya, R. Umino, I. Ohnuma and K. Ishida. High-strength Fe-20Mn-Al-C-based Alloys with Low Density. *ISIJ Int*., 2010, 50, p893-899.

[9] K.H. So, J.S. Kim, Y.S. Chun, K.T. Park, Y.K. Lee and C.S. Lee. Hydrogen Delayed Fracture Properties and Internal Hydrogen Behavior of a Fe-18Mn-1.5Al-0.6C TWIP Steel. *ISIJ Int*., 2009, 49, p1952-1959.

[10] K.T. Park, K.G. Jin, S.H. Han, S.W. Whang, K. Choi and C.S. Lee. Stacking fault energy and plastic deformation of fully austenitic high manganese steels: Effect of Al addition. *Mater. Sci. Eng. A*, 2010, 527, p3651-3661.

[11] J.E. Jin and Y.K. Lee. Strain hardening behavior of a Fe-18Mn-0.6C-1.5Al TWIP steel. *Mater. Sci. Eng. A*, 2009, 527, p157-161.

[12] J.K. Kim, L. Chen, H.S. Kim, S.K. Kim, G.S. Kim. Y. Estrin and B.C. De Cooman. Strain Rate Sensitivity of C-alloyed, High-Mn, Twinning-induced Plasticity Steel. *Steel Res. Int*., 2009, 80, p493-498.

[13] M.M. Nzotta, D. Sichen and S. Seetharaman. Sulphide Capacities in Some Multi Component Slag Systems. *ISIJ Int*., 1998, 38, p1170-1179.

[14] M.M. Nzotta. Experimental Studies of the Sulphide Capacities of MgO-MnO-SiO_2 and MgO-MnO-CaO-SiO_2 Slags. *High Temp. Mater. Process*., 1997, 16, p261-271.

[15] R. Nilsson, M.M. Nzotta, Du Sichen, and S. Seetharaman. Determination of the sulphide capacities of multicomponent slag systems by gas/slag equilibration method. *Proc. 5th Int. Conf. on Molten Slags, Fluxes and Salts*, ISS, Warrendale, PA, 1996, p177-190.

[16] E.T. Turkdogan: *Physical Chemistry of High Temperature Technology*, Academic Press, New York, 1980, p1-26.

[17] www.factsage.com (accessed September 2011).

[18] J.H. Park. Solidification Behavior of Calcium Aluminosilicate Melts containing Magnesia and Fluorspar. *J. Am. Ceram. Soc*., 2006, 89, p608-615.

[19] J.H. Park and Y.B. Kang. Effect of Ferrosilicon Addition on the Composition of Inclusions in 16Cr-14Ni-Si Stainless Steel Melts. *Metall. Mater. Trans. B*, 2006, 37B, p791-798.

[20] J.H. Park. Formation of $CaZrO_3$ at the Interface between CaO-SiO_2-MgO-CaF_2 (-ZrO_2) slags and magnesia refractories: Computational and experimental study. *Calphad*, 2007, 31, p149154.

[21] J.H. Park. Solidification structure of CaO-SiO_2-MgO-Al_2O_3 (-CaF_2) systems and computational phase equilibria: Crystallization of $MgAl_2O_4$ spinel. *Calphad*, 2007, 31, p428-437.

[22] J.H. Park, S.B. Lee and H.R. Gaye. Thermodynamics of the Formation of MgO-Al_2O_3-TiO_x Inclusions in Ti-stabilized 11Cr Ferritic Stainless Steel. *Metall. Mater. Trans. B*, 2008, 39B, p853-861.

[23] M.O. Suk and J.H. Park. Corrosion Behaviors of Zirconia Refractory by CaO-SiO_2-Mgo-CaF_2 Slag. *J. Am. Ceram. Soc.*, 2009, 92, p717-723.

[24] J.H. Park, I.H. Jung and S.B. Lee. Phase diagram study for the CaO-SiO_2-Cr_2O_3-5 mass% MgO-10 mass% MnO system. *Met. Mater. Int.*, 2009, 15, p677-681.

[25] J.H. Park. The effect of boron oxide on the crystallization behavior of $MgAl_2O_4$ spinel phase during the cooling of the CaO-SiO_2-10 mass% MgO-30 mass% Al_2O_3 system. *Met. Mater. Int.*, 2010, 16, p987-092.

[26] J.H. Park, G.H. Park and Y.E. Lee. Carbide Capacity of CaO-SiO_2-MnO Slag for the Production of Manganese Alloys. *ISIJ Int*., 2010, 50, p1078-1083.

[27] J.H. Park and H. Todoroki. Control of $MgO{\cdot}Al_2O_3$ Spinel Inclusions in Stainless Steels - A review. *ISIJ Int*., 2010, 50, p1333-1346.

[28] J.H. Park, J.G. Park, D.J. Min, Y.E. Lee and Y.B. Kang. In situ observation of the dissolution phenomena of SiC particle in $CaO\text{-}SiO_2\text{-}MnO$ slag. *J. Eur. Ceram. Soc.*, 2010, 30, p3181-3186.

[29] J.H. Park, M.O. Suk, I.H. Jung, M. Guo and B. Blanpain. Interfacial Reaction between Refractory Materials and Metallurgical Slags containing Fluoride. *Steel Res. Int.*, 2010, 81, p860-868.

[30] K.Y. Ko and and J.H. Park. Dissolution Behavior of Indium in $CaO\text{-}SiO_2\text{-}Al_2O_3$ Slag. *Metall. Mater. Trans. B*, 2011, 42B, p1224-1230.

[31] J.H. Park. Effect of inclusions on the solidification structures of ferritic stainless steel: Computational and experimental study of inclusion evolution. *Calphad*, 2011, 35, p455-462.

[32] C.J.B. Finchan and F.D. Richardson. Sulphur in silicate and aluminate slags. *J. Iron Steel Inst*., 1954, 178, p4-15.

[33] K.P. Abraham, M.W. Davies and F.D. Richardson. Sulphide capacities of silicate melts, Part I. *J. Iron Steel Inst*., 1960, 196, p309-312.

[34] R.A. Sharma and F.D. Richardson. *Trans. Metall. Soc. AIME*, 1965, 223, p1586-1592.

[35] D.H. Woo and H.G. Lee. Phase Equilibria of the $MnO\text{-}SiO_2\text{-}Al_2O_3\text{-}MnS$ System. *J. Am. Ceram. Soc*., 2010, 93, p2098-2106.

[36] Y.B. Kang and H.G. Lee. unpublished work, private communication, (2011).

[37] L. Pauling. *The Nature of Chemical Bond and the Structure of Molecules and Crystals*, 3rd Ed., Cornell University Press, NY, 1960, p97-102.

[38] Y. Waseda and J.M. Toguri. *The Structure and Properties of Oxide Melts*, World Scientific, Singapore, 1998, p1-4.